

Comparison of Vibration Analysis among NACA Airfoil Wings Based on Natural Frequencies

Zahin Mostakim, Nagib Mehruz, Moaz Ebon Zabal, Kaisar Ahammed Sajib, Md. Zahid Hossain*

Department of Mechanical and Production Engineering, Islamic University of Technology, Gazipur-1704, BANGLADESH

ABSTRACT

In modern aircraft, wings are considered one of the main sources of vibration and noise during the flight. To mitigate this problem, aircraft wing design becomes crucial which largely depends on the selection of airfoil profile and material. Among different airfoil profiles, the NACA series is widely used recently. In this paper, vibration analysis of different NACA series airfoil is performed theoretically using the Euler-Bernoulli beam theory considering the model as a cantilever beam and numerically to determine the natural frequencies and mode shapes of them and finally make a comparison among them based on those determining parameters for NACA 4412, NACA 16-015, and NACA 633-418. Numerical analysis has been performed by ANSYS to determine mode shapes and natural frequencies. The first six mode shapes were extracted. The comparison of natural frequencies among the different NACA series has been shown in this paper.

Keywords: NACA Airfoils series, FEM, Modal Analysis, Natural Frequency, Mode Shape

1. Introduction

Aircraft wings are one of the vulnerable but essential components of airplanes to create required drag and lift forces. It is always under aerodynamic load. So, the safety of aircraft wings is a primary concern in the aviation industry. Vibration analysis of different airfoil wings based on the airfoil is the demand of time. A fundamental way of examining aeroelastic phenomena is to investigate the dynamic characteristics like the natural frequencies and mode shapes. It aids in reducing the noise emitted from the system to the surroundings. It also helps to find out the reasons for vibration which causes damage to the system. Using modal analysis can boost the overall efficiency of the system. This paper is mainly considerate of the numerical modal analysis of the one-dimensional beam model. Models like Euler-Bernoulli and Timoshenko are well-known examples of classical beam models [1].

Many researchers have used one-dimensional beam models to conduct free vibration analysis as the beams are the basic structures of engineering models.

Nikhil A. Khadse & Prof. S. R. Zaveri presented a modal analysis of aircraft wings used for the investigation of NACA 64A215 in their paper. PROE5.0 was used to model the aircraft wing. Modal analysis was performed out by using ANSYS. For the validation of the simulation, a cantilever beam model was used. This study shows that the natural frequency found from the numerical and theoretical methods were similar.[2]

Kakumani Sureka and R Satya Meher modeled A300 aircraft wing using standard NACA 64215 airfoils with spars and ribs digitally using different materials [3] Hrushikesh N et al. performed a harmonic analysis of NACA 4412 for identifying crack [4].

Meral Bayraktar and Ali Demirtaş used NACA 4415 as the root and tip of the airfoil. They used a cantilever beam as a model and calculated theoretical natural frequencies of different modes. Later, ANSYS

software was used to conduct a numerical analysis of the same model to validate the theoretical results. [5]

In this study, natural frequencies of airfoil models of various NACA profiles, like NACA 4412, NACA 16-015, and NACA 633-418, are investigated. For theoretical calculations, the same methodology has been adapted shown by Meral et al. [5]. Here, the full analytical process of NACA 4412 is shown along with the partial calculations of the other two models. ANSYS is used to performed Numerical analysis. Finally, the comparison of the numerical results with theoretical ones among the NACA models has been shown.

2. Airfoil Selection

The curvature of the geometric centerline of the airfoil section and the section's thickness distribution along the span of the airfoil was described by the primary NACA airfoil series that are derived using analytical equations. The later families are derived using theoretical rather than geometrical methods as they are of more complicated shapes.[6]

Terms like maximum thickness, maximum camber, the position of maximum thickness, position of maximum camber, and nose radius can summarize airfoil geometry in Fig. 1. It can be drafted by the coordinates of the upper and lower surface.

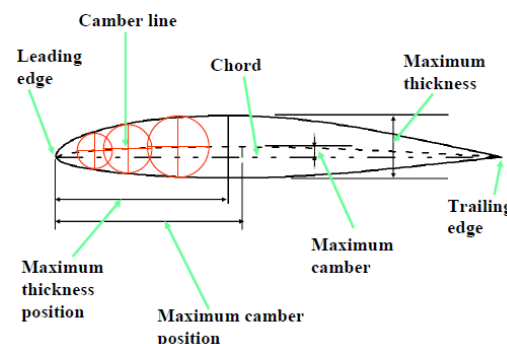


Fig.1 Airfoil Geometry [6]

In NACA 4412, the maximum camber in the percentage of the chord is shown by the first digit, the second digit gives in the tenth of a chord where the maximum camber occurs, and maximum thickness in percentage chord is represented by the last two digits. Airfoil profile of NACA 4412, NACA 16-015, NACA 633-418 is shown in Fig. 2, Fig. 3, and Fig. 4 respectively.

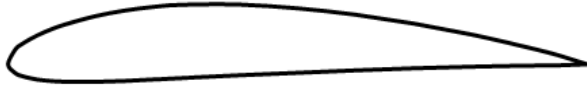


Fig.2 NACA 4412

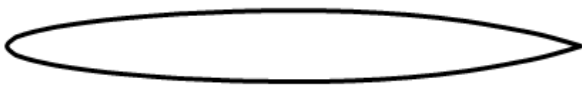


Fig.3 NACA 16-015



Fig.4 NACA 633-418

3. Methodology:

To perform the numerical analysis, first, a 3D design of the airfoil was prepared using SOLIDWORKS. Then, the design was imported to ANSYS for performing finite element analysis to determine the natural frequencies and mode shapes. The meshing is done carefully as the shape of the wing is very complicated. The aluminum alloy 6061 is selected as this material which is commonly used for aircraft wings. Theoretical and numerical analysis is done using modal analysis. The first six modes are extracted from the simulation and comparison of natural frequencies and mode shapes among them are shown in this paper. The numerical and theoretical results are in good agreement. Although, the error percentage increases with the increase of the mode number.

4. Theoretical Calculations

For a cantilever beam, Euler-Bernoulli Beam's theory can be used for finding natural frequencies. In this paper, the aircraft wing is assumed to be a cantilevered beam. The natural frequency equations of Euler-Bernoulli Beam Theory are (Eq.1,2,3) [7]:

$$\omega_n = (\beta_n L)^2 \sqrt{\frac{EI}{mL^4}} \quad (1)$$

Young's Modulus is denoted by E , the moment of inertia is denoted by I , unit mass is denoted by m , and length is denoted by L . Eq. (2) and Eq. (3) is used to calculate $\beta_n L$

$$\frac{d^2}{dx^2} \left\{ EI \frac{d^2 Y(x)}{dx^2} \right\} = \omega^2 m(x) Y(x) \quad (2)$$

$$\beta^4 = \frac{\omega^2 m}{EI} \quad (3)$$

For different mode shapes ($n=1,2,\dots,6$), the value of $\beta_n L$ are calculated in table 1 below:

Table 1 $\beta_n L$ [8]

N	$\beta_n L$
1	1.875
2	4.694
3	7.854
4	10.996
5	14.137
6	17.279

The vertical deviation of an aircraft wing can be measured by using the spanwise bending stiffness distribution along the primary axis of loading. Here, Young's Modulus is considered to be the scaling factor for the specific solid material used for the wing. The upper surface and the lower surface of the wing are generated using the coordinate values from the UIUC airfoil database that are represented by $Y_u(x)$ and $Y_l(x)$ respectively. I is the total bending inertia and A is the cut-section area. As shown in fig. 5, the model is divided into infinitesimal quadrilateral units with width dx and height ($Y_u - Y_l$) that is the difference between the upper surface and the lower surface. [9]

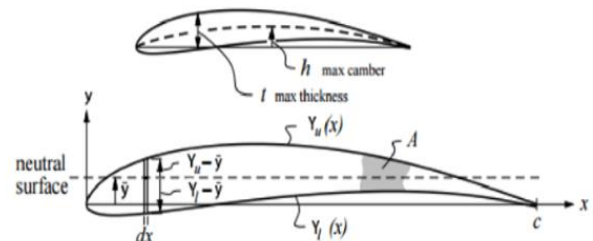


Fig.5 Quantities for calculating bending inertia [8]

Equation 4 to equation 14 is adapted from ref[5] to calculate the bending inertia of the airfoil wing.

$$A = \int_0^c (Y_u - Y_l) dx \quad (4)$$

$$\bar{y} = \frac{1}{A} \int_0^c \frac{1}{2} (Y_u^2 - Y_l^2) \quad (5)$$

$$I = \int_0^c \frac{1}{3} [(Y_u - \bar{y})^3 - (Y_l - \bar{y})^3] dx \quad (6)$$

$$t = \text{maximum} (Y_u(x) - Y_l(x)) \quad (7)$$

$$h = \text{maximum} ([Y_u(x) + Y_l(x)]/2) \quad (8)$$

$$\tau \equiv t/c \quad (9)$$

$$\varepsilon \equiv h/c \quad (10)$$

$$K_A = \frac{1}{c^2\tau} A \int_0^c \{Y_u(x) - Y_l(x)\} dx \quad (11)$$

$$K_I = \frac{1}{c^4(\tau^2 + \varepsilon^2)} \int_0^c \frac{1}{3} [(Y_u - \bar{y})^3 - (Y_l - \bar{y})^3] dx \quad (12)$$

The approximate values of K_I and K_A for the most common airfoils are 0.036 and 0.6 respectively. The moment of inertia I can be calculated as given in Eq. (13) and Eq. (14)

$$A \cong K_A ct \quad (13)$$

$$I \cong K_I ct(t^2 + h^2) \quad (14)$$

4.1 Calculations of NACA 4412 Profiled Wing

The coordinates of the x -axis and y -axis are collected from the UIUC airfoil database and implemented in excel. For x -axis values, $Y_u(x)$ and $Y_l(x)$ were separated where they represent the point values of the upper curve and the lower curve of the airfoil. In table 2, the difference and the average of upper and lower curve points are shown adapted from ref[5].

Table 2 Organized columns from the data of airfoil profile NACA 4412

x axis values	Upper Surface	Lower Surface	Differences	Average
1	0	0	0	0
0.95	0.0147	-0.0016	0.0163	0.00655
0.9	0.0271	-0.0022	0.0293	0.01245
0.8	0.0489	-0.0039	0.0528	0.0225
0.7	0.0669	-0.0065	0.0734	0.0302
0.6	0.0814	-0.01	0.0914	0.0357
0.5	0.0919	-0.014	0.1059	0.03895
0.4	0.098	-0.018	0.116	0.04
0.3	0.0976	-0.0226	0.1202	0.0375
0.25	0.0941	-0.025	0.1191	0.03455
0.2	0.088	-0.0274	0.1154	0.0303
0.15	0.0789	-0.0288	0.1077	0.02505
0.1	0.0659	-0.0286	0.0945	0.01865
0.075	0.0576	-0.0274	0.085	0.0151
0.05	0.0473	-0.0249	0.0722	0.0112
0.025	0.0339	-0.0195	0.0534	0.0072
0.0125	0.0244	-0.0143	0.0387	0.00505
		Maximum	0.1202	0.04

The maximum values found from the last two columns;

$$t=0.1202 \text{ m and } h=0.04 \text{ m}$$

From the design of the wing, we got; cord length $c = 1 \text{ m}$ and wing length $L = 5 \text{ m}$

According to the selected material (Aluminum Alloy 6061) properties of the wing, the following parameters were used;[11]

$$E=69 \times 10^9 \text{ [Pa]} \text{ and } \rho=2700 \text{ [kg/m}^3\text{]}$$

From Eq. (9-14), the following results were obtained shown in table 3 below:

Table 3 Calculated results

Symbols	Values
τ	0.1202 m
ε	0.04 m
A	0.07212 [m ²]
I	6.944 $\times 10^{-5}$ [m ⁴]
M	194.724 [kg/m]

So, the angular natural frequencies were found as;

$$\omega_{nf} = (\beta_n L)^2 \sqrt{\frac{EI}{mL^4}} = (\beta_n L)^2 \sqrt{\frac{69 \times 10^9 \times 6.9443 \times 10^{-5}}{194.724 \times 5^4}} = (\beta_n L)^2 \times 6.275$$

$\omega_{nf} = (\beta_n L)^2 \times 6.27464672$ is used to calculate the natural frequency of each mode is shown in table 4 below.

Table 4 Natural frequency of each mode

Mode	Angular Frequency ω_{nf} [rad/sec]	Natural Frequency f_{nf} [Hz]
1 st	22.062	3.511
2 nd	138.259	22.004
3 rd	387.044	61.600
4 th	758.621	120.738
5 th	1254.054	199.588
6 th	1873.383	298.157

4.2 Calculations of NACA 16-015 Profiled Wing

Following the same procedure;

$$\omega_{nf} = (\beta_n L)^2 \sqrt{\frac{EI}{mL^4}} = (\beta_n L)^2 \sqrt{\frac{69 \times 10^9 \times 0.0001215}{243 \times 5^4}} = (\beta_n L)^2 \times 7.42$$

Using this value to determine the natural frequencies of NACA 16-015 is shown in table 5 below;

Table 5 Natural frequency of each mode

Mode	Angular Frequency ω_{nf} [rad/sec]	Natural Frequency f_{nf} [Hz]
1 st	26.123	4.158
2 nd	163.709	26.055
3 rd	458.290	72.939
4 th	898.266	142.963
5 th	1484.897	236.328
6 th	2218.231	353.042

4.3 Calculations of NACA 633-418 profiled wing
Following the same procedure;

$$\omega_n f = (\beta_n L)^2 \sqrt{\frac{EI}{mL^4}} = (\beta_n L)^2 \sqrt{\frac{69 \times 10^9 \times 0.000213032}{291.5676 \times 5^4}}$$

$$= (\beta_n L)^2 \times 8.981$$

Using this value to determine the natural frequencies of NACA 633-41 is shown in table 6 below;

Table 6 Theoretical Natural Frequencies of NACA 633-418

Mode	Angular Frequency $\omega_n f$ [rad/sec]	Natural Frequency $f_n f$ [Hz]
1 st	31.578	5.026
2 nd	197.898	31.496
3 rd	553.998	88.171
4 th	1085.858	172.819
5 th	1794.999	285.682
6 th	2681.482	426.770

5. Numerical Analysis

5.1 CAD Modelling of Wing

The solid model of an aircraft wing was made using SOLIDWORKS 2016. First, The coordinate (X, Y) values of the airfoil were obtained from the UIUC airfoil site and imported to excel. Another column was added for Z-axis and the values were kept zero. That file was saved in the format text document. Later, a curve was drawn in SOLIDWORKS using the feature “Curve Through XYZ points” using that text file. Then, the curve was converted and the proper dimension of the cord length was given. The extrude boss feature was used to make a 3D model shown in fig. 6 below.

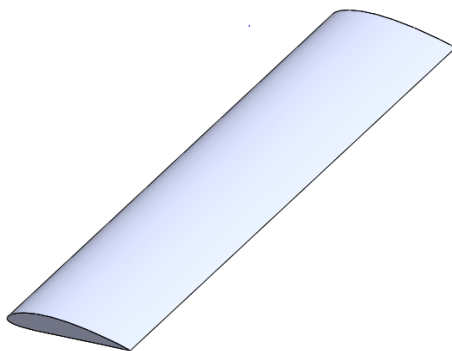


Fig.6 NACA 4412

5.2 Dimensions

Similar to the theoretical analysis, cord length and wing length are taken as 1m and 5m respectively.

5.3 Meshing

The unit cell size of a mesh is very important. The accuracy of the result of the experiment depends on the element size of the mesh. Finer element size enhances the precision of the result, but this requires higher computing power and consumes more time. As the total number of nodes increases with the increase of the total number of element size, the simulation requires solving all those points. Keeping the computing power of the computer used, the mesh was generated shown in fig. 7. Solid 187 was used as an element. The number of elements was 26078 and the number of nodes was 48078.

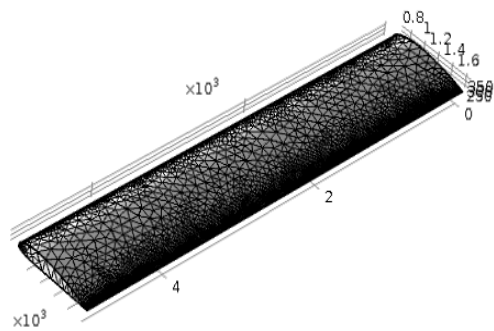


Fig.7 Zoom view of mesh element

5.4 Boundary Conditions

At the Root of the wing, frictionless fixed support was given similar to a cantilever beam. Frictionless support places a normal constraint on the entire surface.

5.5 Material

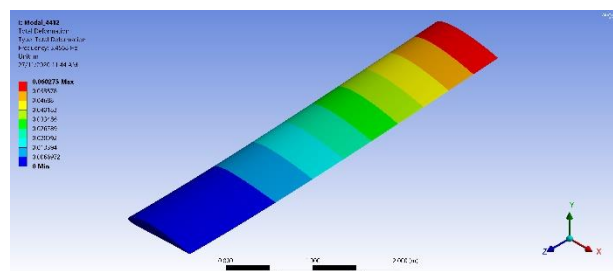
The material selected for this study was Aluminum Alloy 6061 shown in table 7 below.[11]

Table 7 Material properties of Aluminum Alloy 6061

Properties	Values
Young's Modulus	69 GPa
Poisson's Ratio	0.33
Tensile Strength: Ultimate (UTS)	310 MPa
Thermal Conductivity	167 W/m-K
Density	2700 kg/m ³

5.6 Mode shapes of NACA 4412

While running the simulation we set the analysis settings to find the six natural frequencies and their corresponding mode shapes. The results are shown in Fig. 8 below:



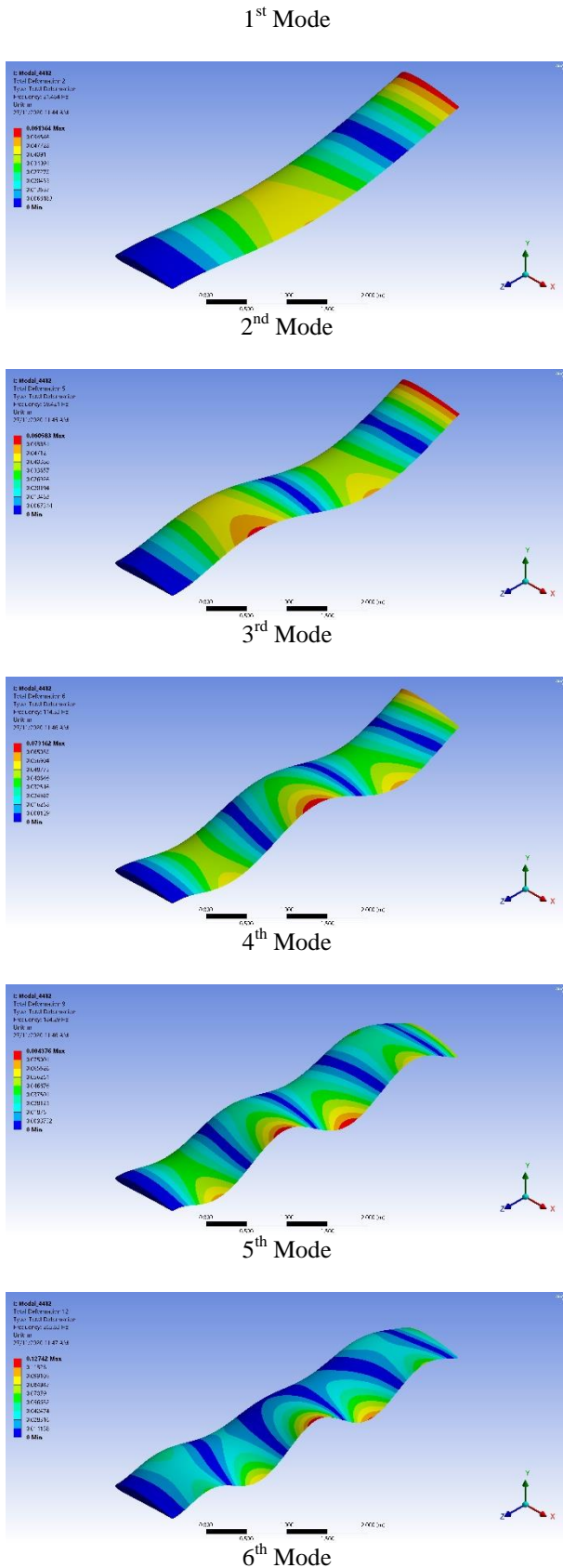


Fig.8 Mode Shapes of NACA 4412

6. Numerical Results

The natural frequencies found in the modal analysis for NACA 4412, NACA 16-015, and NACA 633-048 profiled wings are given below in table 8.

Table 8 Numerical natural frequencies

Modes	Natural Frequencies (Hz)		
	4412	16-015	633-418
1 st	3.4568	4.2172	4.8738
2 nd	21.448	26.281	30.313
3 rd	59.421	73.025	83.906
4 th	114.32	141.32	161.67
5 th	184.29	231.02	261.37
6 th	265.82	339.65	379.26

7. Results and Discussion

7.1 Comparison of results of NACA 4412

Table 9 Comparison between Theoretical and Numerical results of NACA 4412

Mode	Natural Frequencies		Error ratio %
	Theoretical Results	Numerical Results	
1 st	3.511	3.4568	1.544
2 nd	22.004	21.448	2.595
3 rd	61.600	59.421	3.667
4 th	120.738	114.32	5.614
5 th	199.588	184.29	8.301
6 th	298.157	265.82	12.165

7.2 Comparison of results of NACA 16-015

Table 10 Comparison of Theoretical and Numerical Results of NACA 16-015

Mode	Natural Frequencies		Error ratio %
	Theoretical Results	Numerical Results	
1 st	4.158	4.2172	-1.424
2 nd	26.055	26.281	-0.860
3 rd	72.939	73.025	-0.118
4 th	142.963	141.32	1.982
5 th	236.328	231.02	2.298
6 th	353.042	339.65	3.943

7.3 Comparison of results of NACA 633-418

Table 11 Comparison between theoretical and Numerical results

Mode	Natural Frequencies		Error ratio %
	Theoretical Results	Numerical Results	
1 st	5.026	4.8738	3.119
2 nd	31.496	30.313	3.904
3 rd	88.171	83.906	5.083
4 th	172.819	161.67	6.896
5 th	285.682	261.37	9.302
6 th	426.770	379.26	12.527

7.4 Comparison of Numerical Results

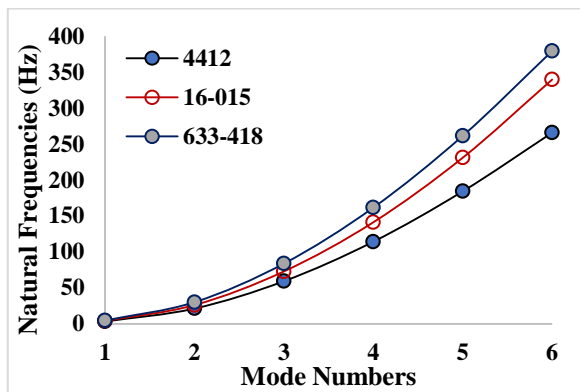


Fig.9 Result Comparison of NACA 4412, NACA16-015, NACA 633-418

7.5 Discussions

In table 9, the first six modes of natural frequencies are presented for the airfoil profile NACA 4412. These frequencies are measured from theoretical and numerical methods. It is found that the theoretical values are higher than the numerical ones. These differences may be due to the empirical formulas used especially for varying cross-sectional areas of airfoils and total inertia. It is clear that the difference between these two methods significantly increases at mode four (5.6%) and reaches the maximum at sixth mode (12.16%). It might be due to meshing quality in higher modes is deteriorated. In table 10 and table 11, natural frequencies of NACA 16-015 and NACA 633-418 are shown. For NACA 16-015, the difference between the two methods is less compare to others. But the pattern is that the difference in natural frequencies increases with the increase of mode number. In fig. 9, it is found that the six-digit NACA airfoil wings have higher natural frequencies than four and five-digits NACA airfoils. This is because of the change in the design of the cord length and cross-section.

8. Conclusions:

In this study, different NACA airfoil models like NACA 4412, NACA 16-015, and NACA 633-418 are investigated theoretically and numerically considering the aircraft wings as a cantilever beam. The results found from both the process are compared. It has been seen that the error is very less in first mode. However, as the mode number increases, the error percentage also increases, but in a reasonable range. Natural frequencies extracted from numerical analysis and theoretical analysis are compared among different models and found in a very good agreement. Natural frequencies of NACA 633-418 are comparatively higher than other models.

Future works: Harmonic analysis will be performed for the same excitation force that is very important to understand that in which model; the vibration effect is lower analyzing the amplitude of vibration.

9. References

- [1] Carrera, E., Petrolo, M., & Varello, A. (2012). Advanced beam formulations for free-vibration analysis of conventional and joined wings. *Journal of Aerospace Engineering*, 25(2), 282-293.
- [2] Khadse NA, Zaveri SR. Modal Analysis of Aircraft Wing using Ansys Workbench Software Package. *International Journal of Engineering Research & Technology (IJERT)*, ISSN. 2015:2278-0181.
- [3] Sureka K, Meher RS. Modeling and structural analysis on A300 flight wing by using Ansys. *International Journal of Mechanical Engineering and Robotics Research*. 2015 Apr 1;4(2):123.
- [4] Hrushikesh N. Paricharak, Aditya A. Lotake, Sudhakar V. Mane, Darshan R. Gaikwad, Rushikesh H. Vastre, Digambar T. kashid, "Analysis of Crack on Aeroplane Wing at Different Positions using ANSYS Software" *International Journal of New Technology and Research (IJNTR)* ISSN: 2454-4116, Volume-5, Issue-4, April 2019 Pages 59-63
- [5] Demirtaş A, Bayraktar M. Free vibration analysis of an aircraft wing by considering as a cantilever beam. *Selçuk Üniversitesi Mühendislik, Bilim Ve Teknoloji Dergisi*. 2019;7(1):12-21.
- [6] Abbott IH, Von Doenhoff AE. *Theory of wing sections: including a summary of airfoil data*. Courier Corporation; 2012 Apr 26.
- [7] <https://www.scribd.com/document/56517062/BIP-OL-1-Handout-8A-1> (25 July, 2019)
- [8] Rao SS. *Vibration of continuous systems*. New York: Wiley; 2007 Mar 23.
- [9] <https://ocw.mit.edu/courses/aeronautics-and-astronautics/16-01-unified-engineering-i-ii-iii-iv-fall-2005-spring-2006/systems-labs-06/spl10b.pdf> (5 August, 2019)
- [10] https://mselig.ae.illinois.edu/ads/coord_database.html (8 April, 2019)
- [11] <http://asm.matweb.com/search/SpecificMaterial.aspx?bassnum=ma6061t6> (15 May, 2019)

NOMENCLATURE

- ω_n : angular natural frequency, rad/sec
 f_n : natural frequency, Hz
 β_n : natural Angle, rad
 L : wing's length, m
 I : total bending inertia, kg/m²
 m : unit mass, kg/m
 $Y_u(x)$: wing's maximum upper surface point, m
 $Y_l(x)$: wing's minimum lower surface point, m
 t : wing's maximum thickness, m
 h : wing's maximum camber, m
 c : chord length, m